CONFERENCE PRE-PRINT

CHARACTERIZATION OF ENHANCED PLASMA PERFORMANCE PHASE AFTER PELLET INJECTIONS IN THE TJ-II STELLARATOR

I. GARCÍA-CORTÉS
Laboratorio Nacional de Fusión
CIEMAT, Av. Complutense 40 28040 Madrid, Spain
Email: Isabel.garciacortes@ciemat.es

K.J. McCARTHY[1], B. van MILLIGEN[1], T. ESTRADA[1], D. MEDINA-ROQUE[1], A. BACIERO[1], A. CAPPA[1], J.M FONTDECABA[1], R. GARCÍA[1], J. HERNÁNDEZ-SÁNCHEZ[1], F.J. HERNANZ[1], F. LAPAYESE[1], D. LOPEZ-BRUNA[1], B. LOPEZ-MIRANDA[1], F. MEDINA[1], J.L. de PABLOS[1], N. PANADERO[1], I. PASTOR[1], A. de la PEÑA[1], P. PONS-VILLALONGA[1], M.C. RODRIGUEZ[1], D. TAFALLA[1] and TJ-II TEAM[1]
Laboratorio Nacional de Fusión
CIEMAT, Av. Complutense 40 28040 Madrid, Spain

V. TRIBALDOS, L. GARCIA, B. CARRERAS
Universidad Carlos III de Madrid
Leganés, Madrid, Spain

B.A. CARRERAS
Department of Physics,
University of Alaska, Fairbanks, Alaska

A. A. CHMYGA, S. KOZACHEK
Institute of Plasma Physics, NSC KIPT
Kharkiv, Ukraine

Abstract

In the TJ-II stellarator, a pellet-induced enhanced-confinement (PiEC) phase is induced by pellet injections into NBI heated plasmas. As a consequence, its operational regime has been extended by up to a factor of 1.5 when compared with fuelling by beam, gas-puff and/or wall recycling. The main characteristics of this PiEC phase are: steepened density gradients, increased ion temperatures, record stored energy and particle confinement times, reduced turbulence, etc. Here, multi-pellet injection studies are extended to a broader range of plasma conditions. For instance, the plasma potential becomes more negative across the whole plasma radius after an initial large PI while additional injections induce steeper dentity gradients and broadened plasma potential profiles. Indeed, when scanning using a HIBP, the radial electric field, E_r, is found to increase in the gradient region at normalized radius of $\rho = 0.6$ from ~-3 kV/m (without pellets) up to ~-8 kV/m (after two pellets) consistent with Neoclassical (NC) simulations. Furthermore, a clear relationship is found also between these observed improvements and the evolution of E_r shear in the region $\rho \sim 0.75$ of the 100_48_65 configuration, as measured by using the Doppler Reflectometer technique. Finally, the impact of the TJ-II rotational transform profile on the quality of PiEC phases has been analysed for the same magnetic configuration by modulating the net plasma current using external field coils. It is found that the radial positioning of low-order rational surfaces near the edge gradient region plays a role in local turbulence suppression, zonal flow generation, and subsequent transport barrier formation. These results are corroborated by Resistive Magneto-Hydrodynamic (MHD) turbulence modelling. In general, pellet injection in TJ-II triggers a new regime driven by the combined effects of reduced turbulence and more favourable neoclassical transport properties, transitioning from Pfirsch–Schlüter to the Plateau regime, leading to a clear enhanced performance.

1. INTRODUCTION

Pellet injection (PI) serves not only serves as a means to fuel the core plasma but it can also lead to improved confinement in both tokamak and stellarator machines [1, 2]. In the TJ-II stellarator, a sustained phase of pellet-induced enhanced confinement (PiEC) is achieved during neutral beam injection (NBI)-heated discharges [3, 4]. Such plasmas exhibit performance enhancements of up to 50% relative to the ISS04 scaling law predictions [5], for instance, record values have been attained in the TJ-II for diamagnetic energy, central electron density, and both central and normalized β when multiple pellets are injected. These discharges in the TJ-II are also marked by a centrally peaked density profile, reduced turbulence levels and elevated ion temperatures. The former effect is

linked to better electron-ion heating transfer [4]. More recently, new work from TJ-II shows that rotational transforms can impact on PiEC quality [6]. In the reported experiments, the net plasma current was controlled using external field coils to modify the rotational transform profile. As a result, the positioning of low-order rational surfaces close to the edge gradient region substantial changes in edge electron density gradients - reaching up to 50 to 60% - and in plasma energy content - ranging from 20 to 30% - were observed. It was postulated therein that such positionings can influence local turbulence levels and can promote the development of zonal flows and associated transport barriers. In general, in the case of PiEC phase while neoclassical (NC) transport modelling may account for part of the experimental observation [7], resistive MHD turbulence [8] and gyrokinetic microturbulence [9] have also been proposed as contributing mechanisms in the transition to this enhanced regime.

Here, we extend the study to a larger database with multi-pellet injections into a range of plasma conditions. We characterize the impact of pellet injection on plasma potential and radial electric field shear, focusing on the onset and development of enhanced confinement phase. Subsequently, by modulating net plasma current, we attempt to understand the role of magnetic topology and how specific rational surfaces can influence PiEC dynamics in TJ-II.

2. EXPERIMENTAL SET-UP

The TJ-II [10] is a 4-period stellarator of the heliac type, with a major radius of 1.5 m and an average minor radius of up to 0.22 m. The plasma volume enclosed by the last-closed magnetic surface (LCFS) reaches up to 1.1 m³, and the on-axis magnetic field can be as high as 1.1 T. Plasmas are generated using microwave heating provided by two gyrotrons operating at 53.2 GHz with a total ECRH power of up to 500 kW. Using this system, plasma discharges can last up to 300 ms, with central electron densities, n_{e0}, and temperatures, $T_e(0)$, up to 1.7×10^{19} m^{-3} and 1.5 keV, respectively, albeit not achieved simultaneously. The corresponding central ion temperature, T_{i0}, remains below or equal to 80 eV. Additional plasma heating is achieved through two tangential neutral beam injection (NBI) systems, which operate in counter- and co-injection configurations relative to the toroidal magnetic field direction. These provide up to ~1 MW of additional power into the vacuum vessel through the NBI ports for up to 120 ms. When the inner wall of the vacuum chamber is coated with boron plus lithium, NBI-heated plasmas of ≤ 120 ms with $n_e(0)$, $T_e(0)$, and $T_i(0)$ up to 8×10^{19} m^{-3}, 400 eV, and 120 eV, respectively, can be achieved with beam plus wall recycling fuelling only.

TJ-II is equipped with an extensive set of diagnostics that enables precise characterization of plasma behaviour and profiles [11]. Among the primary tools, a microwave interferometer provides continuous time-resolved measurements of the line-averaged electron density. The diamagnetic stored energy, W_{dia}, is obtained from a diamagnetic loop. Next, in order to monitor edge and core radiation, Balmer H_α (656.3 nm) detectors are employed alongside a multi-foil soft X-ray system. Electron density and temperature profiles across the plasma radius are acquired using a Thomson Scattering (TS) diagnostic system that provides one profile per discharge. The absolute amplitude of the TS density is calibrated against the line-integrated density obtained with interferometry. Additionally, TJ-II employs a two-channel Doppler Reflectometer (DR) and a dual Heavy Ion Beam Probe (HIBP) system [12, 13]. The DR operates in X-mode with dual-frequency hopping in the 33 GHz to 50 GHz range and variable probing angles up to ±20°, enabling measurement of the radial electric field, E_r, and local turbulence levels at two outer plasma positions. The dual HIBP system is designed to study plasma potential with high spatial (<1 cm) and temporal (1 μs) resolution at two toroidal locations. In nominal set-ups, HIBP-I is fixed at a mid-radius location ($\rho \approx 0.5$–0.7), while HIBP-II operates in scan mode, sweeping from the high-field side ($\rho < 0$) to the low-field side ($\rho > 0$). This set-up facilitates high-resolution measurement of the plasma potential and its fluctuations, while measurement of the secondary ion current is used as an indicator of local plasma density.

In the experiments considered here, hydrogen pellets are injected into the NBI-heated phase of TJ-II discharges that are confined using different magnetic configurations labelled by "xxx_yy_zz" representing currents in the circular, helical, and vertical field coils. The magnetic configurations considered here are 101_40_63 (a = 0.171 m, $\iota_0/2\pi$ = 1.51, V_{plasma} = 1.043 m^3), 101_42_63 (a = 0.191 m, $\iota_0/2\pi$ = 1.534, V_{plasma} = 1.079 m^3), 100_44_64 (a = 0.1925 m, $\iota_0/2\pi$ = 1.551, V_{plasma} = 1.098 m^3) and 100_48_65 (a = 0.191 m, $\iota_0/2\pi$ = 1.591, V_{plasma} = 1.09 m^3) where $\iota_0/2\pi$ is on-axis rotational transform. For these, the volume-averaged magnetic field strength, $\langle B \rangle_{vol}$, is between ~0.93 T and ~0.96 T. Plasmas, with hydrogen as the working gas, are created using electron cyclotron resonance heating (ECRH) and once developed additional heating, provided by one or both NBIs, is injected. With regard to PI, a pellet injected into ECRH plasma is typically fully ablated before reaching the plasma centre ($\rho = 0$). The result is a transient increase in plasma line-averaged density, $\langle n_e \rangle$, and a post-injection pellet particle deposition profile that is rather flat with no significant changes in plasma performance. In contrast, the pellet ablation rate is significantly lower for NBI-heated plasma due to reduced T_e; thus, pellets can penetrate beyond the magnetic axis.

However, because of strong radial drifting of ablated material in TJ-II, post-ablation pellet particle deposition tends to occur in the plasma core for deep pellet penetration (NBI-heated plasmas) and close to the outer edge for shallow penetration (ECRH plasmas). In this work we will focus in the evolution of the plasma potential, E_r and its shear in the enhanced confinement phase after PI characterized mainly by the dual-HIBP and the DR systems.

3. EXPERIMENTAL RESULTS

During recent TJ-II experimental campaigns, significant efforts were made to characterize this PiEC phase for different plasma conditions. A significant database has been analysed to identify how deep core fuelling induces a clear enhanced performance in NBI plasmas. Fig. 1 shows experimental energy confinement time (τ_E) versus energy confinement time expected from the ISS04 scaling law (τ_E^{ISS04}) [5]. For this, injected NBI heating power is in the range (400 to 900 kW, Co/Cntr), plasma wall conditioning is used (boron and/or lithium coating) and 4 magnetic configurations are selected: 101_40_63, 101_42_63, 100_44_65 and 100_48_65. The target density for pellet injection is in the range 1 to $2x10^{19}$ m^{-3} and two or more pellets are injected with a separation time $\Delta t \approx \tau_E$ in order to optimize the PiEC phase. Black points are for plasmas fuelled by beam and/or wall recycling while coloured points are for plasmas with PI(s) (one, two or three pellets). Current datasets confirm the results from [3, 4], enhancements in τ_E of approximately 50% are achieved relative to the τ_E^{ISS04} empirical law (dash line in Fig. 1) following multiple pellet injections for high heating power and different magnetic configuration. This enhancement factor, on the order of 1.5, currently defines the upper bound achieved for pellet-fuelled plasmas heated by NBI in TJ-II, where it is clear that core fuelling is the key parameter to induce an enhanced plasma phase and extend the TJ-II operational regime by such factors.

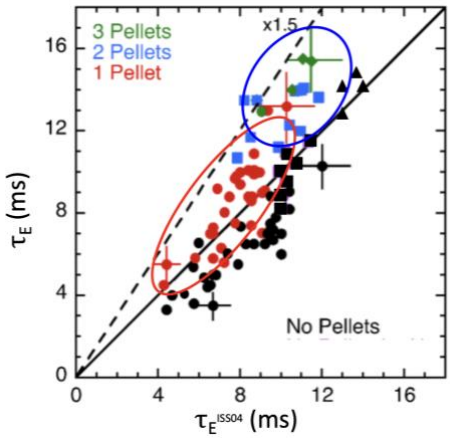

FIG. 1: Diamagnetic energy confinement time, τ_E, versus predicted ISS04 times, τEISS04, for selected plasmas. This is an extension of figure in ref. [4] for a larger database. Data points are for a range of NBI-heating powers, different magnetic configurations and plasma-wall conditionings. The points represent no PI (black dots), 1 PI (red dots), 2 PIs (blue squares) and 3 PIs (green diamonds). Error bars are included for selected data.

3.1. The impact of pellet injection on the plasma potential, radial electric field and its shear

The plasma potential profile is a key parameter for understanding the physics underlying this PiEC phase. In order to investigate potential profiles after PIs with comparable densities, we select a set of reproducible TJ-II discharges with and without PI in which the plasma density increases steadily along the NBI heating phase.

Fig. 2 shows the time evolution of global plasma parameters for two shots where plasmas were created in the 100_44_64 configuration with 220 kW of ECRH, which was switched off at 1140 ms, while 440 kW of co-counter NBI was applied from 1130 to ~1240 ms. Two pellets were injected during the NBI-heated phase in discharges #55318, whereas discharge #55298 was fuelled by the beam and by wall recycling, thereby inducing a near linear increase of density. The former is used as a reference shot. In #55318, the pellets penetrated the plasma edge at 1160 ms and 1175 ms, with each one being ablated fully within ~300 μs. In the

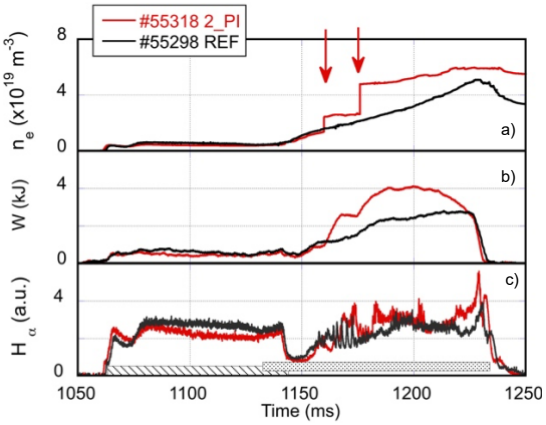

FIG. 2. Traces of line-averaged electron density, ne, stored plasma diamagnetic energy, W, and Balmer Ha emission for TJ-II discharges #55298 (black) and #55318 (red). Pellet injections are made into discharge #55318 at 1160 ms and 1174 ms. NBI only heating is employed from 1140 ms to 1230 ms.

plot, each pellet produces a prompt rise in line-averaged density as well as a significant increase in stored energy W_{dia}, thereafter reaching a PiEC plateau (4 kJ) that last about 40 ms (1180 to 1220 ms, ~ 3 τ_E). Also observed is a reduction in H_α, especially after the second pellet, this indicating better plasma-wall interaction compared to that of the reference discharge. With regard to density and temperature profiles, Thomson Scattering profiles show that the impact of PI on temperature profile is minimal, i.e., central T_e (~300 eV) drops by less than 10% after PI whereas the n_e profile is increased mainly in the plasma centre, *i.e.*, from $4x10^{19}$ m^{-3} in the reference shot up to $6x10^{19}$ m^{-3} after 2 PIs. It has to be noted that T_i increases up to 200 eV in core after PI in discharge from the same series as #55318 (see Fig. 7 in Ref [4]).

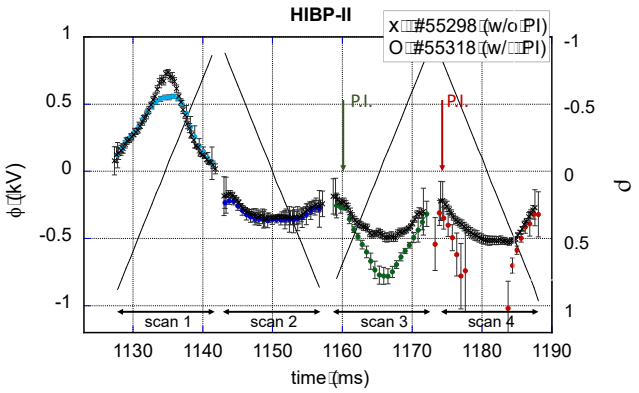

FIG. 3. Plasma potential profiles (left axis) for TJ-II discharges #55298 (reference, crosses) and #55318 (2 pellet injections, circles) obtained using the HIBP scan mode. Vertical arrows indicate the times when pellets are injected into discharge #55318. Scans are made for 4 different phases along these discharges: ECRH phase (scan1, light blue), initial NBI-heated phase (scan 2, dark blue dots), mid NBI-heated phase (scan 3, green dots) and final NBI-heated phase (scan 4, red dots). Grey lines indicate the radial position (right axis) of the HIBP beam as a function of time. Error bars represent the point dispersion for each measurement.

In TJ-II, its dual HIBP system can measure the plasma in detail at fixed positions or measure across the whole plasma radius by scanning its beam. Fig. 3 shows the time evolution of plasma potential for the same shots as in Fig. 2. The plasma potential is measured by sweeping the primary ions of the HIBP-II system to explore the region $-0.9 < \rho < 0.9$ every 15 ms (see Fig. 3, right y-axis). In Fig. 3, full potential profiles can be seen for four different plasma phases for both a reference discharge (#55298, represented by crosses) and for a discharge with PI (#55318, represented by full circles). In the initial discharge stage, the potential profile for purely ECR heated plasma, (scan 1 for 1125 ms to 1140 ms) is positive for both cases as the plasma is in electron-root. Next, the potential becomes negative as the plasma transits from the electron-root to ion-root during the initial NBI heating phase after ECRH is switched-off, (scan 2 for 1143 ms to 1158 ms). Both discharges present similar potential profiles during these scans. Then, in the third phase, (scan 3 for 1160 ms to 1175 ms), a pellet is injected at t = 1160 ms for shot #55318. It is seen for this phase that the plasma potential shows more negative values after the pellet injection than for the reference shot across the whole plasma volume, but especially in the plasma core where a difference of ~ -300 V is observed. In the last phase, (scan 4 for 1175 ms to 1190 ms), after a second pellet is injected into discharge #55318, the potential becomes more negative with respect to the reference than during the third scan phase. It should be noted that as density increases to maximum TJ-II values, it is not possible to make measurements in the centre due to beam attenuation. Also, the error bars for the plasma potential increase due to the reduced current of Cs^{2+} ions collected by the HIBP-analyser. In summary, a pellet injection into NBI-heated plasmas induces a more negative plasma potential in the whole plasma volume that becomes more negative as additional pellets are injected.

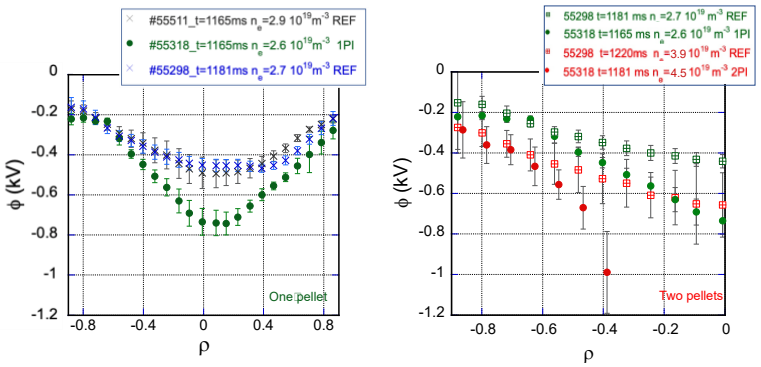

FIG. 4: Plasma potential profiles obtained using the HIBP-II system. Left: profiles for 3 low-density plasmas (see insert): #55318 (green points) after 1 pellet injection plus #55298 (blue crosses) and #55511 (black crosses) without pellet injection. Right: Plasma potential profiles for low-density and high-density phases of #55318 (green points after 1 PI, red points after 2 PIs) and #55298 (green squares for low-density, red squares for high density). Error bars represent the dispersion in each measurement.

Next, since density in the reference shot #55298 ramps up along the discharge (see Fig. 2a), it provides a good framework to compare plasma potential profiles for low and high plasma densities with and

without pellet injections. In Fig. 4, potential profiles for plasmas with and without pellet injection are compared for low-density and high-density cases. It is evident that for similar low densities, the potential profile is more negative if a pellet injection is performed. This would indicate that, in TJ-II, central pellet depositions enhance the electric field in the gradient region, for instance, E_r ~-3 kV/m for the reference plasma while E_r = ~-5 kV/m at ρ = 0.5 after a pellet injection even though densities are similar. Moreover, as shown also in Fig. 4, the potential profile broadens and becomes more negative when an additional pellet is injected, compared to both a single pellet case and to a beam/edge-fuelled plasma of similar density. Thus, as determined from HIBP signals in TJ-II, the estimated E_r is significantly more intense in the PiEC phase of a high-density plasma than in a standard high-density plasma (E_r ~-4 kV/m at ρ = 0.6 for the reference compared to E_r = ~-8 kV/m after 2 PIs).

Furthermore, in order to characterize the evolution of the radial electric field shear in the gradient region we use the two channel Doppler Reflectometer (DR) for a series of reproducible discharges into which one, two or three pellets were injected, consecutively. These shots were produced in the 100_48_64 configuration with 440 kW of co-counter NBI heated power. Fig. 5 shows the E_r shear (dE_r/dr) at ρ = 0.75 obtained from DR measurements made at ρ = 0.7 and 0.8. It is seen how dE_r/dr becomes more negative after each consecutive pellet. For instance, after the first pellet, Fig. 5a, the shear becomes more negative than the reference value and remains so for several ms. After the second pellet, Fig. 5b, the shear becomes more negative than the shear induced by the first pellet before returning towards the reference level after ~20 ms. In contrast, the injection of the third pellet maintains this negative E_r shear at maximum level (-200 kV/m) until the end of the shot, Fig. 5c, this coinciding with increased stored plasma energy, as can be deduced from Fig. 5d. Thus, in these experiments, a clear relationship is found between improved plasma performance and the evolution of E_r shear in the gradient region. For these same discharges, a more negative E_r is determined from HIBP scanned plasma potentials with E_r at ρ = 0.75 being -2.5 kV/m for the reference and -6 kV/m after two pellets are injected.

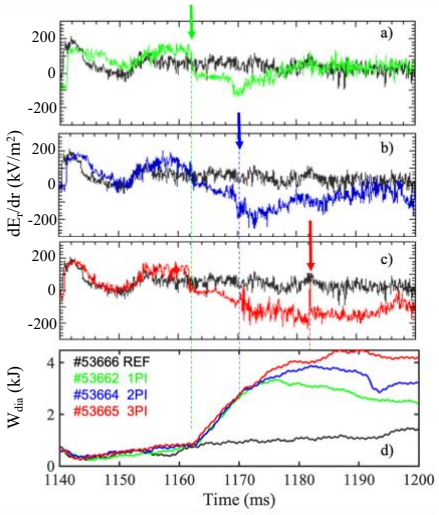

FIG. 5: a-c) the time evolution of the E_r shear (dE_r / dr) ρ ~ 0.75 along four TJ-II discharges with 1, 2, 3 or no pellets: arrows indicate when the first (green), second (blue) and third (red) are injected. d) time evolution of stored energy for the same discharges, reference (black), 1 PI (green), 2 PIs (blue) and 3 PIs (red). All shots in configuration 100_48_65.

When density profiles of these same discharges are studied, it is found that the gradient becomes progressively steeper for ρ < 0.7 after each consecutive pellet injection (Fig. 6 left) while the electron temperature (Fig. 6 right) reduces slightly in the bulk plasma, ρ < 0.5, after each pellet. The development of an enhanced gradient in density points to the formation of a transport barrier associated with the increased E_r shear around ρ = 0.75. This close correspondence between the evolution of the shear, the steepening of the density profile together with the enhanced confinement suggests that pellet injections not only supply particles to the plasma but also reinforce shear-induced confinement in the gradient region.

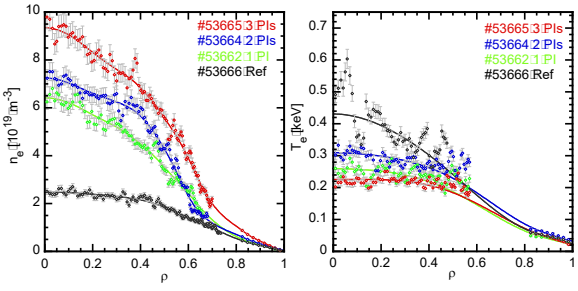

FIG. 6: TS profiles and fitted curves for ne (left) and T_e (right) for the same discharges as in Fig. 5. Reference #53666 (black), with 1 PI #53662 (green), 2 PIs #53664 (blue) and 3 PIs #53665 (red). The TS is set at 1191.4 ms for #53666, at 1171.4 ms for #53662, at 1181.4 ms for #53664 and at 1191.4 ms for #53665. All shots are made in the configuration 100_48_65.

3.2. The impact of the magnetic topology on pellet-induced enhanced confinement in TJ-II

In order to understand better the role of magnetic topology during the PiEC phase, experiments were conducted for series of NBI-heated discharges created using the same magnetic configuration, 100_48_65, while varying the net plasma current, I_p. See Fig. 7. This configuration was selected as its vacuum rotational transform profile shows low rational surfaces at, or close to, the LCFS. TJ-II is characterized by its low-shear helical-axis design which implies that its rotational transform profile can be strongly affected by small variations in net plasma current. Thus, by systematically varying the current through the external ohmic field coils, the rotational transform profile is modified and the radial positions of the low rational surfaces of interest are moved radially inwards or outwards. See Fig. 7. In these experiments, in which I_p was swept from -2 kA to +4 kA, the 3/2, 8/5, and 5/3 rational surfaces are displaced radially inside the LCFS. Modified iota-profiles were obtained using VMEC calculations for low induced-plasma currents and it is found that predictions are in good agreement with experimental cross-checks made by HIBP scans and Mirnov coil analysis [6] as well as by the interpretation of structures observed in pellet ablation profiles [14]. In the experiments, post-injection density profiles show a clear increase in the edge gradient, see Fig. 8, and significant confinement improvements after PIs as I_p becomes more negative or positive (Fig. 8). For instance, electron density gradients increase by 50% to 60% in the region inside $\rho = 0.8$, and the plasma energy content improves by 20% to 30%, when low-order rational surfaces are placed in the same radial region. DR measurements made for these discharges indicate reduced turbulence levels and enhanced zonal flows in the vicinity of such rational surfaces while E_r profiles (Fig 8) display systematic variations as plasma current is varied, thereby supporting the hypothesis that these features facilitate transport barrier formation.

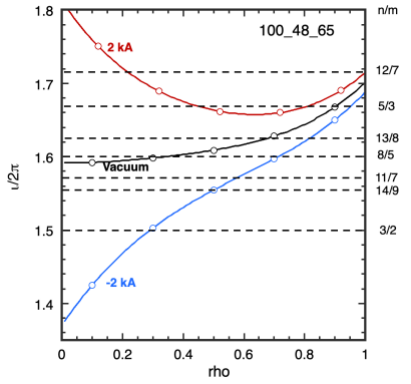

FIG. 7: Rotational transform profiles for configuration 100_48_65 in vacuum and for two non-zero values of I_p, according to the model in Ref [9]. Rationals, $\iota = n/m$, in the range 1.5 to 1.8 with $n > 15$ are highlighted as dash-dash lines.

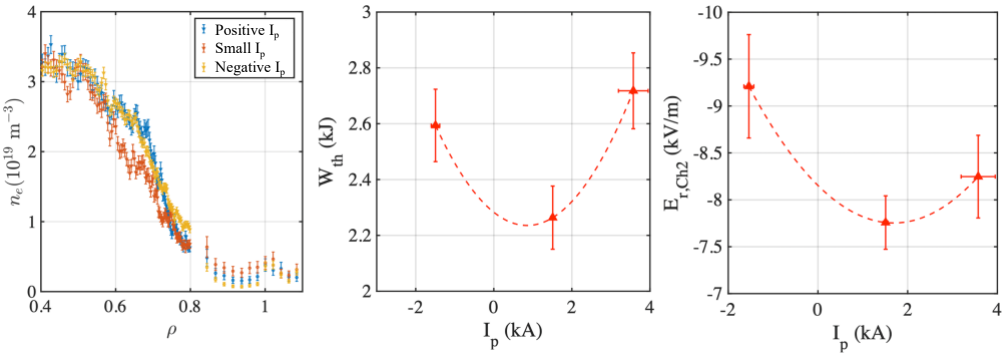

FIG. 8: Left: Density profiles measured after pellet injection using the Thomson Scattering (TS) and He-beam systems for discharges with different net plasma current (blue is negative I_p, red is near zero Ip, yellow is positive Ip). Centre: thermal plasma energy versus I_p for the same discharges. Right: Radial electric field, Er, at $\rho \sim 0.7$ (from 2-channel Doppler reflectometer) versus I_p for the same discharges. Dash-dash lines are used to guide the eye for W_{th} and E_r. The horizontal axis corresponds to the measured value of net plasma current, I_p (kA), when the TS measurement is made.

Resistive MHD turbulence simulations [6] have been carried out for injections into these plasmas, *i.e.*: for positive, negative and near zero plasma currents. The main conclusions from performing such simulations are as follows. For positive currents (~+2 kA) alignment of the 5/3 rational surface was found to enhance confinement through the formation of dual transport barriers and significant turbulence suppression, accompanied by the generation of strong zonal flows. In contrast, for negative currents (~-2 kA), it is possible to highlight the interplay between the various low-order rational surfaces that are predicted to be present, *i.e.*, 3/2, 8/5, and 5/3, which improves the confinement by enhancing long-range coupling and suppressing turbulence further. At small currents, the effect of rational surfaces appears weaker, with limited changes to the rotational transform profile leading to reduced transport barriers and less pronounced confinement improvements.

4. NEOCLASSICAL SIMULATIONS

In order to evaluate the role of neoclassical (NC) transport in the PiEC phase, NC simulations has been carried out for three shots of the same series that discharges in Fig. 2, shot without pellets #55298, with one pellet injection #55313 and with two pellets #55300. A combination of MOCA and DKES codes were employed to study transport characteristics [7]. The main finding is that the substantial rise in ion temperature (due to better electron-ion energy transfer) reduces ion collisionality, thereby mitigating neoclassical diffusion and driving the transition from the Pfirsch–Schlüter (plasmas without pellets) to the Plateau regime (for the plasmas with one and two pellets). Furthermore, results for E_r exhibits an increase to more negative values for the two pellets case in reasonable agreement with experimental measurements shown in the previous section, thereby further supporting the interpretation that pellet injection reduces NC transport and contributes, in part, to the observed confinement improvement.

5. SUMMARY

In summary, we have extended multi-pellet injection studies to a broader range of plasma conditions to high power heating and different magnetic configuration. The main result is that the previous enhancement factor, on the order of 1.5, currently defines the upper bound achieved for pellet-fuelled plasmas heated by NBI in TJ-II, where it is clear that core fuelling is the key parameter to induce an enhanced plasma phase and extend the TJ-II operational regime by such factors. In dedicated experiments, we also observe that the plasma potential becomes more negative across the whole plasma radius after PI and the injection of additional pellets induces broader plasma potential profiles. These have been observed at low and high density when compared with similar discharges without pellet injections. Moreover, as a consequence, E_r increases in the gradient region from about -5 kV/m (without pellets) up to -8 kV/m (after two pellets) at $\rho \sim 0.5$ for discharges with similar densities, indicating that core fuelling by pellets induces less negative radial electric fields. These are experimental observations made using HIBP methods, and compatible with E_r from NC simulations [7]. Furthermore, it is also observed that multi-pellets keep the E_r shear at maximum level, this being coincident with longer energy confinement times. There is a close correspondence between the evolution of the shear, the steepening of the density profile together with the enhanced confinement suggesting that pellet injections also reinforce shear-induced confinement in the gradient region and transport barrier formation. Finally, the impact of the rotational transform profile of TJ-II on the quality of PiEC phases has been analysed in detail by modulating the net plasma current using external field coils. The findings reveal that the radial positioning of low-order rational surfaces near the edge gradient region play a role in the local turbulence suppression, zonal flow generation, and subsequent transport barrier formation. These results are corroborated by Resistive Magneto-Hydrodynamic (MHD) turbulence modelling.

Overall, pellet injection in TJ-II NBI plasmas not only enhances electron-to-ion energy transfer but also triggers a confinement improvement regime driven by the combined effects of reduced turbulence [8, 9] and more favorable neoclassical transport properties [7], leading to experimental enhancement of plasma performance.

ACKNOWLEDGEMENTS

This work has been carried out within the framework of the EUROfusion Consortium, funded by the European Union via the Euratom Research and Training Programme (Grant Agreement No 101052200 - EUROfusion). Views and opinions expressed are however those of the author(s) only and do not necessarily reflect those of the European Union or the European Commission. Neither the European Union nor the European Commission can be held responsible for them. In addition, it is partially financed by grants from the Spanish Ministerio de Ciencia e Innovación (PID2020-116599RB-I00, PID2021-125607NB-I00 and PID2023-148697OB-I00). The authors acknowledge the contributions to HIBP data collection, analysis and interpretation made by A. Melnikov, M. Drabinskiy, L. G. Eliseev, and P. Khabanov as part of the long-term trilateral collaboration between National Research Center 'Kurchatov Institute', Moscow, Russia, led by S. Melnikov, the HIBP group from Kharkov Institute of Physics and Technology, Kharkov, Ukraine, led by L.I. Krupnik, and CIEMAT.

REFERENCES

[1] LANG, P.T., BLANKEN, T. C., DUNNE, M., McDERMOTT, R. M, et al., Feedback controlled, reactor relevant, high-density, high-confinement scenarios at ASDEX Upgrade, Nucl. Fusion 58 (2018) 036001.

[2] BALDZUHN, J., DAMM, H., BEIDLER, C. D., McCARTHY, K. J., et al., Enhanced energy confinement after series of pellets in Wendelstein 7-X, Plasma Phys. Control. Fusion 62 (2020) 055012.

[3] GARCÍA-CORTÉS, I., McCARTHY, K. J., ESTRADA, T., TRIBALDOS, V., et al., Enhanced confinement induced by pellet injection in the stellarator TJ-II, Phys. Plasma 30 (2023) 072506.
[4] McCARTHY, K. J., GARCÍA-CORTÉS, I., ALONSO, J. A., ARIAS-CAMISÓN, A., et al., Multi-pellet injection into the NBI-heated phase of TJ-II plasmas, Nucl. Fusion 64 (2024) 066019.
[5] YAMADA, H., HARRIS, J. H., DINKLAGE, A., ASCASÍBAR, E. et al. Characterization of energy confinement in net-current free plasmas using the extended International Stellarator database, Nucl. Fusion 45 (2005) 1684.
[6] van MILLIGEN, B., GARCÍA-CORTÉS, I., McCARTHY, K. J., CARRERAS, B. A., et al. The rotational transform and enhanced confinement in the TJ-II stellarator, J. Plasma Phys. 91 (2025) E98.
[7] TRIBALDOS, V., GARCÍA-CORTÉS, I., McCARTHY, K. J., REYNOLDS-BARREDO, J. M., et al, Confinement modelling of enhanced plasma performance after multipellet injection in the TJ-II stellarator, 30th IAEA FEC 2025.
[8] GARCÍA, L., GARCÍA-CORTÉS, I., CARRERAS, B. A., McCARTHY, K. J., et al., The effect of pellet injection on turbulent transport in TJ-II, Phys. Plasma. 30 (2023) 092303.
[9] GARCÍA-REGAÑA J.M., and TJ-II TEAM, Transport in high-performance plasmas of the TJ-II stellarator: From first principles to experimental validation, at this conference.
[10] HIDALGO, C., ASCASÍBAR, E., ALEGRE, D., ALONSO, A., et al., Overview of the TJ-II stellarator research programme towards model validation in fusion plasmas, Nucl. Fusion 62 (2022) 042025.
[11] McCARTHY, K., and TJ-II TEAM, Plasma diagnostic systems and methods used on the stellarator TJ-II, J. Instrum. 16 (2021) C12026.
[12] HAPPEL, T., ESTRADA, T., BLANCO, E., TRIBALDOS, V. et al, Doppler reflectometer system in the stellarator TJ-II, Rev. Sci. Instrum. 80 (2009) 073502
[13] MELNIKOV, A.V., KRUPNIK, L. I., ELISEEV, L. G., BARCALA, J. M. et al., Heavy ion beam probing diagnostic to study potential and turbulence in toroidal plasmas, Nucl. Fusion 57 (2017) 072004.
[14] MCCARTHY, K. J., GARCÍA-CORTÉS, I., van. MILLIGEN, B., BACIERO, A., et al., Interpreting structures observed in pellet ablation profiles in the stellarator TJ-II, at this conference.